Journal of Catalysis **188,** 281–290 (1999)
Article ID jcat.1999.2666, available online at http://www.idealibrary.com on IDEAL®

Effect of Water Vapor on the Reduction of Ru-Promoted Co/Al_2O_3

Yulong Zhang,[1] Dongguang Wei,[2] Sonia Hammache, and James G. Goodwin, Jr.[3]

Department of Chemical and Petroleum Engineering, University of Pittsburgh, Pittsburgh, Pennsylvania 15261

Received March 16, 1999; revised August 17, 1999; accepted August 18, 1999

The effect of water vapor on the reduction of a calcined Ru-promoted Co/Al_2O_3 catalyst was investigated by introducing water vapor during the standard reduction procedure (H_2, 350°C, 10 h) and during TPR. The presence of added water vapor (up to 3%) during standard reduction resulted in a decrease in the amount of Co able to be reduced. A peak located at ca. 500°C was observed in the TPR profiles of the catalyst after standard reduction in the presence of water. The amount of cobalt reducible in this temperature range increased with water vapor concentration. The reduction of this cobalt species, which was probably due to Co interacting strongly with the Al_2O_3, was inhibited during standard reduction in the presence of water vapor. Addition of water vapor during standard reduction also led to a decrease in the total amount of reducible cobalt (<900°C). The "nonreducible" cobalt existed mainly in the form of a cobalt aluminate with a reduction temperature higher than 900°C during TPR. It was observed that introduction of water vapor during TPR of the calcined catalyst also had a significant effect on the TPR profile. Two peaks could be observed in either the presence or the absence of added water vapor. The first reduction peak at ca. 230°C remained essentially unchanged; however, the second reduction peak temperature (400–600°C) shifted up to 200°C higher and the peak area decreased to ca. one-third in the presence of increased water vapor pressures. The amount of cobalt able to be reduced during TPR to 900°C decreased with an increase in the amount of H_2O added. The presence of water vapor during reduction appears to retard the reduction process by increasing the Co–alumina interaction and/or forming cobalt aluminates.

Key Words: **cobalt; Co/Al_2O_3; temperature-programmed reduction; reducibility; water vapor; Fischer–Tropsch.**

INTRODUCTION

Supported cobalt catalysts are the preferred catalysts for the synthesis of heavy hydrocarbons from natural gas-based syngas because of their high Fischer–Tropsch (FT) activity, selectivity for linear hydrocarbons, and low activity for the water–gas shift reaction (1, 2). It is well known that the reduced Co metal, rather than its oxides or carbides, is the most active phase for CO hydrogenation (3). Investigations have been done on the nature of cobalt species on various supports: alumina (5–13), silica (11, 12, 14–26), titania (11–12, 14, 27), magnesia (11, 12, 28), carbon (11, 12, 29), zeolites (30, 31).

The reducibilities of various cobalt species in supported cobalt catalysts have been studied by TPR, XRD, EXAFS, ESR, FTIR, etc. (4–6, 16–17, 20–23). They can be affected by composition (17), support (11, 12, 14), preparation procedure (9, 19, 25), and pretreatment (5, 7, 32). Many authors (4, 5) have noted that compound formation between cobalt metal and the support can occur under reaction conditions. This is a possible deactivation route due to a decrease in the amount of metallic Co available in the catalyst.

The impact of water concentration on catalyst performance has been investigated due to the high water concentrations that can exist at high reactant conversions. It has been discovered that the presence of water vapor during reaction can enhance the deactivation of cobalt catalysts due to surface oxidation or compound formation between the metal and the support (4, 5). The formation of cobalt silicates on Co/SiO_2 under hydrothermal conditions was extensively studied by Kogelbauer *et al.* (4). Hydrothermal treatment at 220°C led to a catalyst with lower reducibility due to the formation of both reducible and essentially nonreducible (at temperatures < 900°C) Co silicates. It was found that hydrothermal treatment of the reduced catalyst or hydrothermal treatment of the calcined catalyst in the presence of hydrogen produces Co silicates, while hydrothermal treatment of the calcined catalyst in air does not result in their formation. Hydrothermal treatment of the calcined catalyst in inert gas also has little effect.

The deactivation of Al_2O_3-supported cobalt Fischer–Tropsch catalysts as a result of the presence of water vapor during Fischer–Tropsch synthesis (FTS) has been studied by Schanke *et al.* (5). They found that oxidation of the supported cobalt is limited to the surface layers if H_2 is present during hydrothermal treatment. They also reported that a noble metal-promoted Co/Al_2O_3 catalyst has a more rapid deactivation than an unpromoted catalyst. Several

[1] Permanent address: Department of Chemistry, Tongji University, Shanghai, 200092, Peoples Republic of China.

[2] Permanent address: Institute of Coal Chemistry, Chinese Science Academy, Taiyuan, 030001, Peoples Republic of China.

[3] To whom all correspondence should be addressed.

0021-9517/99 $30.00

studies using steady-state isotopic transient kinetic analysis (SSITKA) have shown that the deactivation caused by water vapor being present does not alter the turnover frequency, but decreases the number of active intermediates leading to products (33, 34).

Cobalt catalysts are usually calcined and then reduced by H_2 before reaction to produce higher Co dispersions. The reduction process produces water as the oxygen in the cobalt oxides reacts with hydrogen. If reduction of the catalyst is carried out in a large, deep-bed reactor, a high concentration of water vapor can result at the outlet of the reactor. Until recently, studies of the effect of water vapor on reduction of cobalt catalysts were rare. Holmen and co-workers (5, 8) noted that the relative reaction activity on Re-promoted Co/Al_2O_3 decreased to one-half with water vapor treatment before reaction. They also noted that the reduction of Co/Al_2O_3 in TPR is promoted by wetting a mixture of loose mechanically mixed Co/Al_2O_3 and Re/Al_2O_3 before reduction. It was suggested that water may enhance the interaction between cobalt and Re.

Zielinski (43, 44) has studied the effect of water vapor on the reducibility of SiO_2- and Al_2O_3-supported nickel oxide. He found that nickel oxide is reduced in the same way as unsupported nickel oxide in the absence of water, and in a similar way to nickel hydrosilicates in the presence of water. TPR peaks were affected by the addition of water vapor.

In this paper, we address the impact of water vapor on the reducibility of $CoRu/Al_2O_3$ during reduction. Of particular interest is the interaction between cobalt and the Al_2O_3 support resulting from the presence/absence of water vapor. It is well known that the active phase in cobalt Fischer–Tropsch catalysis is cobalt metal. However, spinel cobalt aluminate can be formed during pretreatment, reduction, and catalytic reaction. The spinel cobalt aluminate cannot be reduced to cobalt metal under normal reduction conditions. Obviously, spinel cobalt aluminate formation results in fewer surface cobalt metal atoms available for FTS. In this investigation, effects of water vapor during both standard reduction and TPR were studied. Significant changes in the reducibility of cobalt species and in the TPR profiles were observed as the concentration of water vapor was varied. The effect of water vapor in terms of thermodynamics, kinetics, and phase transformations is discussed.

EXPERIMENTAL

Catalyst Preparation

The Ru-promoted Co/Al_2O_3 catalyst was prepared by the incipient wetness technique. The Al_2O_3 support used was prepared from Vista B. The support precursor was calcined at 500°C for 10 h, producing γ-Al_2O_3 having a specific surface area of ca. 200 m^2/g and an average particle size of ca. 60 μm. Cobalt nitrate and ruthenium nitrosyl nitrate were dissolved in deionized water and coimpregnated into γ-Al_2O_3 to form a catalyst with 20 wt% Co and 0.5 wt% Ru on γ-Al_2O_3. The catalyst was dried at 110°C for 12 h and calcined in air at 300°C for 2 h.

Standard Reduction in the Absence/Presence of Water Vapor

Standard reduction of the catalyst was performed employing a H_2 flow (100% H_2, 30 ml/min) in an Altamira AMI-1 system using a temperature ramp from ambient to 350°C at 1°C/min and holding at 350°C for 10 h. The amount of catalyst used was 50 mg for each run. To investigate the effect of water vapor on reduction, water vapor was introduced into the system by a syringe pump or a saturator. When a syringe pump was employed, the water was introduced into a line heated to ca. 250°C to guarantee its steady evaporation. Deionized water was used that had been deoxygenated by bubbling Ar through it for 2 days. The system lines were heated to ca. 120°C to avoid condensation of water in the system. All the gases used were 99.999% purity and further purified by oxygen traps and silica gel/5A zeolite to exclude trace oxygen and water. Pulse oxygen titration was conducted at 400°C to measure the degree of reduction after the standard reduction. TPR was also performed after standard reduction using ramping from 350 to 900°C at 5°C/min to investigate the changes in the reducibility of the catalyst. These last two procedures were performed in separate experiments.

TPR in the Absence/Presence of Water Vapor

TPR was also carried out in the Altamira AMI-1 system. It was conducted using 50 mg of calcined catalyst and temperature ramping from 30 to 900°C at 5°C/min. The carrier gas was 5% H_2 in Ar. A cold trap (−70°C) was placed before the detector to remove H_2O produced during TPR. The consumption of hydrogen in the TPR process was recorded by a thermal conductivity detector (TCD). The hydrogen consumption measurement was calibrated by TPR of silver oxide (Ag_2O) under the same conditions. For studying the effect of water concentration on TPR, a syringe pump or a water saturator was placed just before the reactor and a U-tube containing silica gel was placed before the cold trap to avoid ice blockage of the flow system. When the syringe pump was used, the water was injected into a line heated to 250°C to ensure evaporation. All system lines were heated to ca. 120°C to avoid condensation of water vapor.

X-Ray Diffraction

A Phillips X'pert System X-ray diffractometer instrument with monochromatized Cu$K\alpha$ radiation was used for the XRD measurements. The spectra were scanned at a rate of 2.4°/min. The average Co_3O_4 crystallite size of the

calcined catalyst was calculated using the Sherrer equation to be 230 Å. After reduction in the absence or presence of water vapor, the samples were flushed with Ar for 30 min and cooled down to room temperature in an Ar stream. Then, they were placed into a container containing liquid paraffin to prevent their oxidation prior to XRD.

Chemisorption

Chemisorption was performed with a Micromeritics ASAP 2010C system. The standard reduction was carried out for the calcined catalyst in the system. After reduction, the catalyst was evacuated at 350°C for 90 min to desorb the chemisorbed H_2. The measurement of hydrogen chemisorption was conducted at 100°C with an equilibrium interval of 180 s. After the first set of hydrogen chemisorption meaurements, the catalyst was soaked in H_2 at 100°C for 30 min; then the system was cooled down to room temperature to measure the reversible uptake. The adsorption isotherms were obtained by the increasing pressure method. The pressure range used was 75 to 500 mm Hg. Extrapolation of the total and reversible adsorption isotherms to zero pressure gave the total uptake and reversible uptake for chemisorbed hydrogen. The "irreversible" chemisorption uptake was calculated from the difference between the total and reversible uptakes. Average particle size of the Co metal in the catalysts was calculated by assuming a stoichiometry of $H_{irr}/Co_s = 1$, an average Co atom surface area (in a plane) of 6.62 $Å^2$, and spherical Co particles with a density of 8.9 g/cm^3. After standard reduction, the average Co metal particle size determined by H_2 chemisorption was 218 Å.

RESULTS

Effect of Water Vapor on Standard Reduction

After standard reduction, the amount of Co able to be reduced during standard reduction in the absence or presence of added water vapor was determined by pulse oxidation at 400°C (see Table 1). In separate experiments, TPR was carried out to measure the amount of additional Co species able to be reduced up to 900°C. TPR profiles after standard reduction in the presence of various water partial pressures are shown in Fig. 1. As can be seen in Table 1, in the absence of added water vapor, 92% of Co was able to be reduced during standard reduction, with only 3.9% additionally reduced during TPR to 900°C. It can be seen in Fig. 1 that the peak around 500°C increased with increasing water partial pressure during the standard reduction process. As reported in the literature (8, 13, 35), the peak around 500°C in TPR of noble metal-promoted Co/Al_2O_3 catalyst is due to the reduction of small particles of amorphous Co species interacting with the support. The presence of water vapor during standard reduction obviously increases the concentration of these cobalt species. It can be seen from Fig. 2 that the amount of this ca. 500°C reducible species increased more quickly at lower water concentrations. The temperature of this TPR peak remained essentially constant (Fig. 3) for all the water concentrations. Introduction of water vapor decreased the degree of reduction of cobalt during standard reduction as well as the total amount able to be reduced up to 900°C (Table 1). The degree of reduction decreased from 92 to 45% after introduction of 3% water vapor in the standard reduction process. Approximately 25% of Co was able

TABLE 1

Effect of Water Vapor on the Degree of Reduction during Standard Reduction[a]

H_2O added					% Reduction[b,c]			
Ramping			Holding					
P_{H_2O} (atm × 100)	% H_2O	H_2O/H_2 ratio	P_{H_2O} (atm × 100)	H_2O/H_2 ratio	During standard reduction[d]	During TPR[e] (350–900°C) after standard reduction	Total[f] (30–900°C)	% Nonreducible (<900°C)
0	0	0	0	0	92	3.9	95.9	4.1
0.6	0.6	0.006	0.6	0.006	67	7.2	84.2	15.8
1.2	1.2	0.012	1.2	0.012	50	18.1	68.1	31.9
1.68	1.68	0.017	1.68	0.017	NA	19.7	NA	NA
3	3	0.031	3	0.031	45	25.3	70.3	29.7
3	3	0.031	0	0	77	NA	NA	NA
0	0	0	3	0.031	69	NA	NA	NA

[a] Standard reduction: ramping from ambient temperature to 350°C at 1°C/min, holding at 350°C for 10 h, pure H_2 with added water at 30 cm^3/min flow rate, total pressure of 1 atm.

[b] Based on complete reduction of 20 wt% Co on the catalyst with Co_3O_4 as the calcined cobalt species.

[c] Error = ±5% of measurement.

[d] Measured by pulse oxidation at 400°C.

[e] Measured by TPR after standard reduction.

[f] Total reduction up to 900°C: measured by sum of the results of pulse oxidation and TPR.

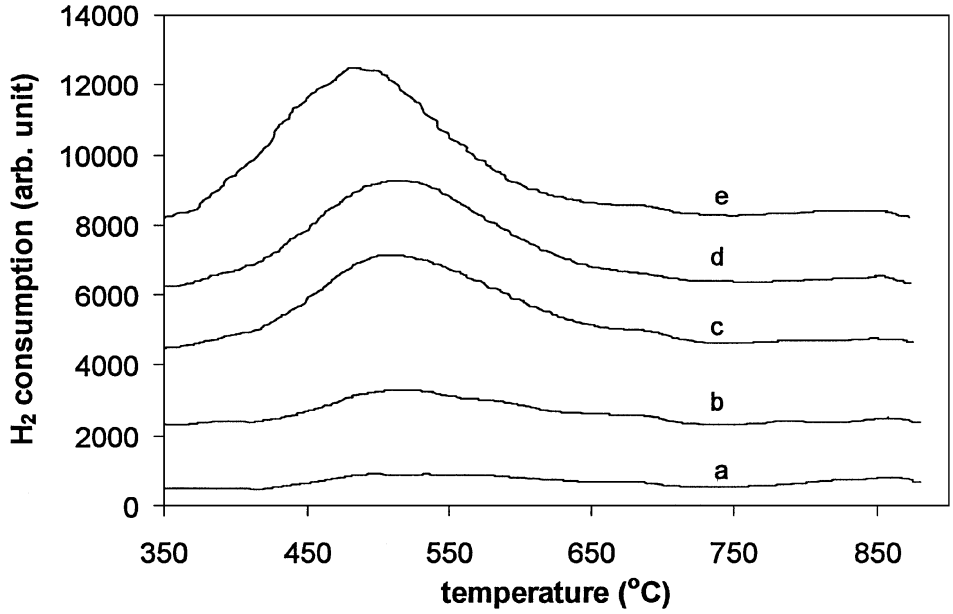

FIG. 1. TPR profiles after standard reduction in the presence of added water vapor. Concentration of water vapor in pure H_2 during standard reduction at 350°C: (a) 0%, (b) 0.6%, (c) 1.2%, (d) 1.6%, (e) 3.0%.

to be additionally reduced during TPR to 900°C, while, ca. 30% remained as nonreducible cobalt species. Introduction of water vapor to the system during both the ramping and the holding periods had a significant influence on the degree of reduction of cobalt. However, introduction of water only to either the temperature ramp or the temperature-holding period of the standard reduction procedure produced just a partial decrease in the reducibility.

Effect of Water Vapor on TPR

To study further the impact of water vapor on reduction of the cobalt catalyst, water vapor was added during TPR of the calcined catalyst. As far as we can ascertain, this is the first reported attempt to study the impact of water vapor during TPR of Co catalysts. The results are very interesting. There were two major peaks located at ca. 250 and ≥500°C in the TPR profiles (Fig. 4), designated as peaks 1 and 2. It can be clearly seen that the TPR profiles changed dramatically after introduction of a small amount of water vapor, especially for peak 2. Figure 5 shows the peak temperatures of TPR as a function of water concentration. The temperature of peak 1 remained essentially the same,

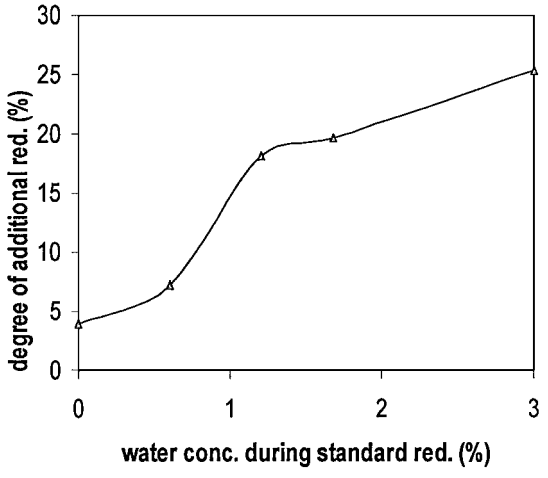

FIG. 2. Effect of water vapor concentration on degree of reduction during TPR after standard reduction in the presence of water vapor.

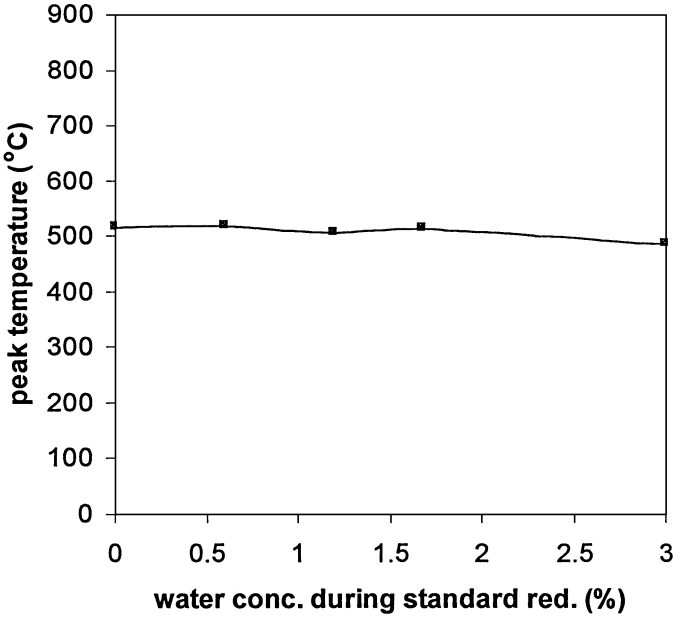

FIG. 3. Effect of water vapor concentration during standard reduction on the peak temperature during subsequent TPR.

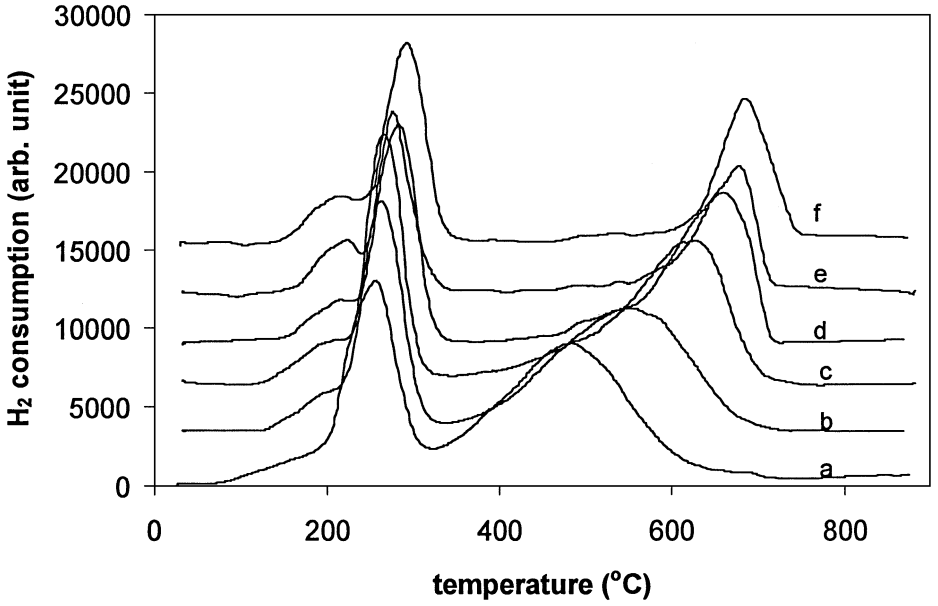

FIG. 4. TPR profiles for the calcined catalyst in the presence of various concentrations of water: (a) 0%, (b) 0.6%, (c) 1.2%, (d) 6.9%, (e) 13.8%, (f) 20.7%.

while that of peak 2 increased with increasing water partial pressures. The shift was more dramatic at lower water partial pressures. The degree of reduction of cobalt during TPR in the presence of the various water vapor concentrations is shown in Fig. 6. It can be seen that water vapor had little impact on the amount of Co reduced at the lower temperature (peak 1). The total degree of reduction and the degree of reduction during peak 2 decreased with increasing water partial pressure. Figure 7 shows the cumulative degree of reduction at various temperatures as a function of water vapor concentration.

Standard reduction leads to a 92% degree of reduction (Table 1). This is achieved during TPR in the absence of added water on reaching ca. 550°C. It can be thus supposed that the degree of reduction reached at 550°C during TPR is comparable to the degree of reduction during a standard reduction at 350°C for 10 h. From Fig. 7 it can be seen that, at 550°C, the degrees of reduction at 0.6 and 1.2% water concentrations are 70 and 50%, respectively. This is consistent with the results in Table 1. The results for TPR in the presence of water vapor are summarized in Table 2.

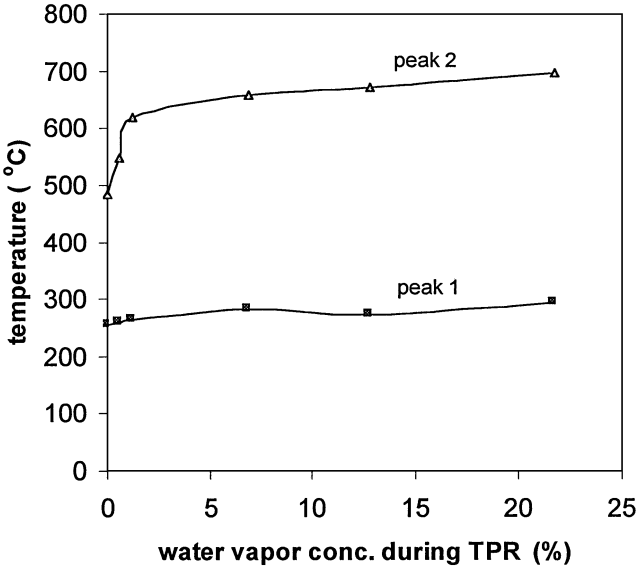

FIG. 5. Effect of water vapor concentration on peak temperatures during TPR of the calcined catalyst.

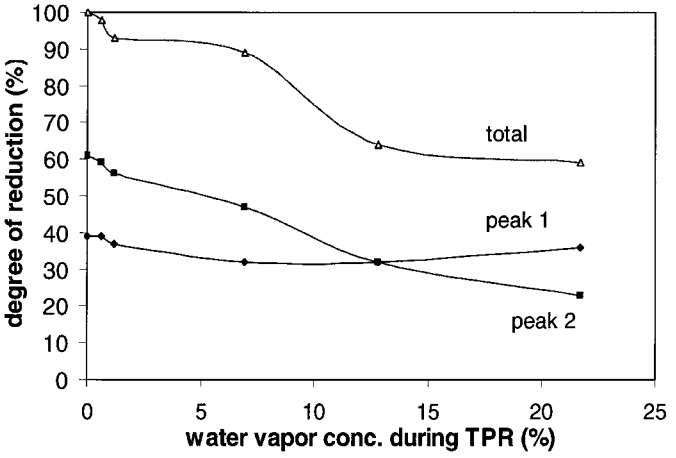

FIG. 6. Effect of water vapor concentration on degree of reduction during TPR of the calcined catalyst.

TABLE 2

Degree of Reduction during TPR in the Presence of Water[a]

Catalyst	% H_2O	H_2O partial pressure (atm × 100)	H_2O/H_2	TPR Peak 1 T (°C)	TPR Peak 1 % Reduction[b,c]	TPR Peak 2 T (°C)	TPR Peak 2 % Reduction[b,c]	Total % reduction[b,c] (30–900°C)
Co_3O_4	0	0	0	300[d]	25	372	75	100
	3.0	3.0	0.6	333	24	397	76	100
$CoRu/Al_2O_3$	0	0	0	255	39	483	61	100
	0.6	0.6	0.12	259	39	547	59	97
	1.2	1.2	0.24	264	37	619	56	93
	6.9	6.9	1.2	283	32	659	47	90
	13.8	13.8	2.55	272	32	672	31	63
	20.7	20.7	4.14	293	36	696	23	59

[a] Carrier gas: 5% H_2 in Ar, $T = 30$–900°C, ramp rate = 5°C/min, calcined catalyst.
[b] Based on complete reduction of the cobalt with Co_3O_4 as the original cobalt species.
[c] Error = ±5% of measurement.
[d] Shoulder.

For comparison, the results for TPR of unsupported Co_3O_4 are also included. The presence of water vapor had little impact on either peak temperature or degree of reduction for TPR of unsupported Co_3O_4.

XRD Measurement

XRD patterns for the $CoRu/Al_2O_3$ catalyst after different treatments are shown in Fig. 8. It can be seen that XRD for calcined $CoRu/Al_2O_3$ was similar to that for unsupported Co_3O_4 with some small contribution from the γ-Al_2O_3. After completion of peak 1 in TPR (stopping TPR at 400°C), diffraction peaks at 31.4° and 59.4° for Co_3O_4

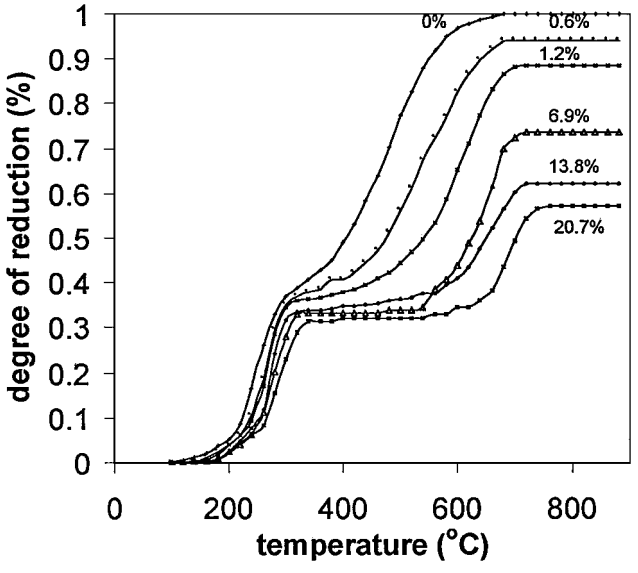

FIG. 7. Cumulative degree of reduction with temperature for various added water vapor concentrations during TPR of the calcined catalyst.

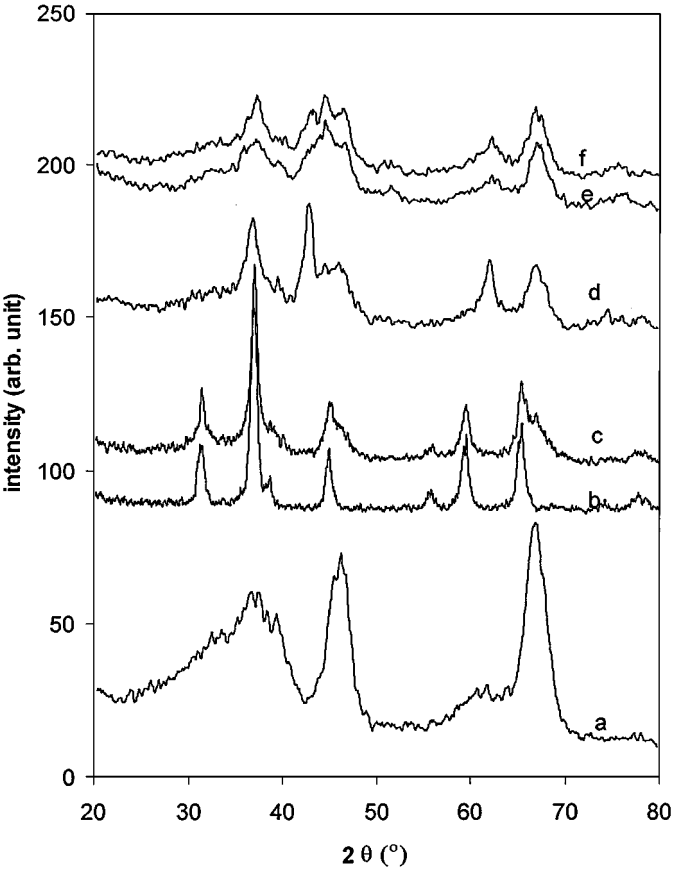

FIG. 8. XRD patterns: (a) γ-Al_2O_3 support, (b) unsupported Co_3O_4, (c) calcined catalyst, (d) catalyst after completion of peak 1 for TPR in the absence of added water vapor, (e) catalyst after standard reduction in the absence of added water vapor, (f) catalyst after standard reduction in the presence of 3% added water vapor.

disappeared. Instead, diffraction lines at 42.4° and 61.5° for CoO appeared. After standard reduction of the catalyst, diffraction peaks for Co_3O_4 disappeared (Figs. 8e and 8f). Compared with the XRD pattern for the partially reduced catalyst during TPR (Fig. 8d), the diffraction lines for CoO decreased greatly. It can be seen from Fig. 8 that the XRD patterns are similar for the catalyst after standard reduction in the absence and presence of added water vapor. However, perhaps a little more CoO phase may have been present for the sample reduced in the presence of added water vapor. Diffraction due to cobalt metal could not be resolved because of broadening and overlapping with the diffraction peaks of γ-Al_2O_3 and CoO phases. An XRD pattern for cobalt aluminate spinel was not observed, suggesting that any cobalt aluminate present was in a highly dispersed state.

DISCUSSION

The origin of the TPR peaks observed for a calcined alumina-supported Co catalyst has been discussed in several papers (8, 13, 35). The lower-temperature peak is usually assigned to reduction of crystalline Co_3O_4 particles. The higher-temperature peak is attributed to the reduction of highly dispersed amorphous cobalt oxide which is interacting strongly with the alumina support. These reduction peaks are shifted to lower temperatures by introducing a small amount of noble metal, such as Ru, as a reduction promoter (4, 38–40).

The peak assignment, however, is still somewhat controversial due to the complexity of the reduction of cobalt catalysts. To clarify the identity of the reduction peaks in TPR for Co/Al_2O_3 catalysts, XRD measurements were conducted with the catalyst after completion of peak 1. It can be seen from Fig. 8d that diffraction peaks for Co_3O_4 disappeared, while diffraction peaks for CoO appeared after completion of peak 1 during TPR. This indicates that Co_3O_4 in the catalyst is reduced to CoO during peak 1 of TPR. Table 2 shows that H_2 consumption for peak 1 of the catalyst during TPR in the absence of added water vapor is much larger than that required for reduction of Co_3O_4 to CoO (equivalent to 25% reduction). It is suggested that reduction of some CoO to Co metal also takes place during peak 1, probably that existing in the large particles of cobalt.

Thermodynamic calculations were carried out using Aspen to explain the effect of water vapor on the reducibility of the cobalt catalyst. The calculated results are shown in Fig. 9. It can be seen that the degree of reduction decreases with increasing H_2O/H_2 ratio and temperature. However, thermodynamically, the effect of water vapor on the reduction of Co_3O_4 is very small. The near-total reduction of bulk Co_3O_4 in H_2 is essentially feasible even in the presence of large amounts of water vapor. The results of TPR

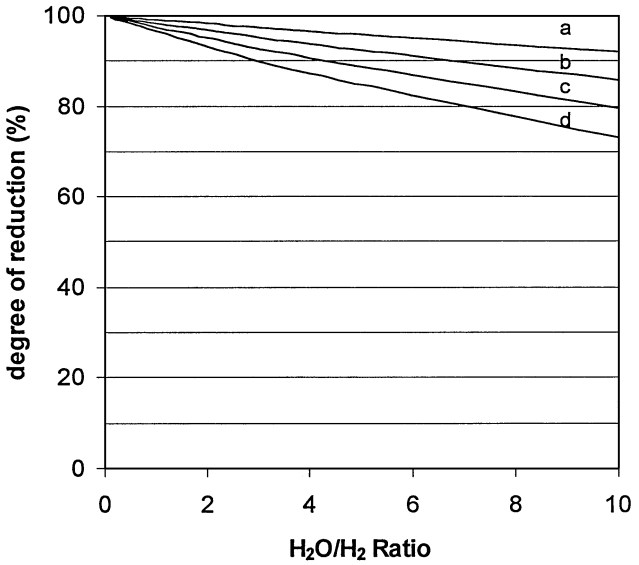

FIG. 9. Thermodynamic limitations to reduction of Co_3O_4 as a function of H_2O/H_2 ratio at various temperatures: (a) 200°C, (b) 400°C, (c) 600°C, (d) 800°C.

for unsupported Co_3O_4 are consistent, as expected, with the thermodynamic predictions.

Usually, the particle size distribution of high-metal-loading catalysts are bimodal rather than single modal. This 20 wt% Co catalyst was no exception, possessing both very large and small particles as evidenced by SEM (TEM is not useful for such a high loading of metal) and the results from H_2 chemisorption and XRD giving average Co_3O_4 (calcined catalyst) and Co (reduced catalyst) particle sizes. The reduction of a fraction of the cobalt present as large particles of Co_3O_4 on the $CoRu/Al_2O_3$ catalyst during the reduction procedure used can be concluded, based on the reduction results and their low interaction with the Al_2O_3 support, to not have been significantly affected by thermodynamic limitations even with the added water vapor. This fraction of the cobalt probably reduced during peak 1 of TPR of the calcined catalyst and during standard reduction with or without added water.

The results obtained (Table 1), however, show that the presence of water vapor during standard reduction did have significant effects on the degree of reduction of the cobalt catalyst and on the subsequent reducibility of the standard reduced catalyst during TPR up to 900°C. The first effect relates to the formation of cobalt species able to be reduced during the following TPR (350–900°C). It is evident from Fig. 1 that the temperature of the reduction peak of this species (ca. 480–510°C) did not change significantly for different water vapor concentrations. Comparing this temperature with the TPR profile in the absence of water vapor (Fig. 4), it can be observed that the peak temperature in Fig. 1 (TPR after standard reduction) is similar to the temperature of peak 2 for TPR of the calcined catalyst in

the absence of water vapor in Fig. 4. This suggests that the reducible cobalt species in the successive TPR after standard reduction in the presence of water vapor is similar to that reduced during peak 2 in TPR of the calcined catalyst in the absence of water vapor. The amount of this cobalt species remaining after standard reduction in the presence of water vapor increases with increasing water vapor concentrations (Fig. 2). It is suggested that the presence of water vapor has a strong inhibitive effect on the reduction of this species during standard reduction.

Another effect of the presence of water vapor during standard reduction is the formation of species that are nonreducible during the following TPR from 350 to 900°C. This nonreducible (<900°C) cobalt is concluded to be in the form of a cobalt aluminate. It can be seen from Table 1 that the amount of nonreducible cobalt species (cobalt aluminate) increases greatly on the addition of small concentrations of water vapor during standard reduction.

The decrease in degree of reduction during standard reduction in the presence of water vapor could be due to kinetic and/or thermodynamic limitations on the reduction of the highly dispersed cobalt species. These Co species (Co_3O_4, CoO, etc.) can have a strong interaction with the γ-Al_2O_3 support. From thermodynamic calculations discussed above, the thermodynamic limitations on the reduction of Co_3O_4 (in the absence of alumina) are essentially negligible. However, the reduction of well-dispersed cobalt species interacting with the support is a different case. Thermodynamic calculations for such a system are difficult because the Co species are not well defined and sufficient thermodynamic data are not available. Thus, a basis does not exist for concluding whether thermodynamic or kinetic limitations apply. However, we strongly hypothesize that the presence of water vapor during standard reduction enhances the equilibration of the interaction of Co with alumina.

Usually, TPR is performed using a small H_2 concentration (ca. 5%) mixed with argon or nitrogen (41). During TPR, water is formed and is purged by the carrier gas. The concentration of water in the reactor during TPR is, thus, very low, and the reduction proceeds under nonequilibrium conditions. Various parameters (H_2 concentration, amount of catalyst, ramping rate, flow rate, etc.) for TPR have been studied (41, 42). However, studies of the effect of H_2O, which is the only product of TPR, on TPR are few. Zielinski (43, 44) has reported the effect of water vapor on the TPR of silica- and alumina-supported nickel catalysts. The effect of water vapor during TPR of supported cobalt catalysts has not been previously reported. In our study, it was found that water vapor has a significant influence on the TPR profiles (Fig. 4). The shoulder of peak 1 became a distinctly separate peak as the main part of peak 1 shifted slightly to higher temperatures with the addition of water. This phenomenon can also be observed in the TPR of unsupported Co_3O_4 as

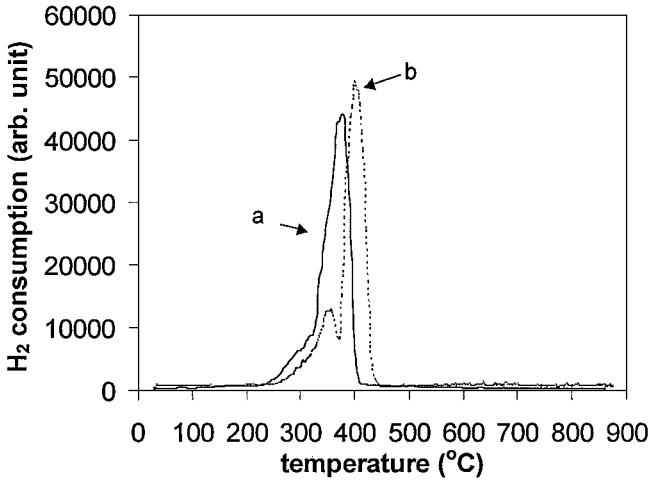

FIG. 10. Effect of water vapor on TPR profiles for unsupported Co_3O_4: (a) 0%, (b) 3%.

shown in Fig. 10. Thus, the effect of water vapor on peak 1 of TPR on $CoRu/Al_2O_3$ is comparable to that on unsupported Co_3O_4. Since the ratio of the areas of these two peaks formed by introducing water vapor into the system in the TPR of unsupported Co_3O_4 approaches 1/3 (the theoretical ratio of H_2 consumption for reduction of Co^{3+} to Co^{2+} and Co^{2+} to Co metal), this pair of peaks can be ascribed to the reduction of Co^{3+} to Co^{2+} and Co^{2+} to Co metal. The similar effect during water addition on peak 1 for TPR of $CoRu/Al_2O_3$ and for the TPR of unsupported Co_3O_4 suggests that this Co species is similar to unsupported Co_3O_4. The reduction of ruthenium oxide cannot be seen in the TPR spectra because of its low relative loading (0.5 wt% Ru) compared with that of Co (20 wt%). XRD results in Fig. 8 also suggest that partial reduction of Co_3O_4 to CoO takes place in peak 1. The dramatic influence of water vapor presence on peak 2 of TPR for $CoRu/Al_2O_3$ indicates that the reduction properties of the cobalt species in peak 2 are different from those of Co_3O_4. It, therefore, must be some type of cobalt species interacting with the alumina support.

The effect of water vapor on the position of peak 2 of TPR for calcined $RuCo/Al_2O_3$ (Fig. 4) probably has two mechanisms. At lower water vapor concentrations, there is a dramatic shift in the peak temperature. This is possibly due to the change or modification of the cobalt species caused by presence of water vapor. Only a slight additional shift was observed at higher water vapor concentrations. A computer simulation of TPR based on the model proposed by Malet and Caballero (42) suggests that a 10–15°C shift in peak temperature could have resulted due to the 20% variation in H_2 concentration and total flow rate with the addition of water vapor. Thus, the slight shifts observed for peaks 1 and 2 at higher water vapor pressures (Figs. 4, 5) as well as the shift for unsupported Co_3O_4 were probably

due only to the small changes in H_2 concentration and total flow rate. It can be noted that the peaks became narrower in the presence of water, and the onset of peak 2 shifted to a higher temperature. The onset temperature represents the initial formation of crystal nuclei of cobalt metal from cobalt species represented by the peak. Therefore, it can be postulated that the presence of water vapor during reduction may have affected the kinetics of crystal nucleation of small cobalt metal particles. It can be seen from Table 2 that the total degree of reduction up to 900°C decreased greatly with increasing water vapor concentration. It is suggested that water facilitates interactions between cobalt species and the γ-Al_2O_3 support to form irreducible cobalt aluminate. It was observed that the catalyst turned dark blue after TPR in the presence of higher water vapor pressures, while it remained black in the absence of added water vapor. The former result is suggestive of cobalt aluminate formation. A similar effect of water vapor on SiO_2-supported nickel catalysts has been observed by Zeilinski (43). He suggested that water vapor and the silica support jointly interact with nickel oxide, probably to form hydrosilicates, and thus retard the reduction of Ni.

Interaction of cobalt and alumina has been observed by many authors (4–13) using various techniques including TPR, XRD, EXAFS, and XPS (ESCA). The migration of cobalt ions into the alumina lattice sites of octahedral or tetrahedral symmetry is limited to the first few layers of the support under normal calcination conditions (6). The γ-Al_2O_3 crystal structure is that of a spinel with a deficit of cations (36). Diffusion of cobalt ions into tetrahedral sites of γ-Al_2O_3 can form a "surface spinel" in Co/Al_2O_3 catalysts. The "surface spinel" structure cannot be observed by X-ray diffraction because it does not have long-range, three-dimensional order (6, 37). It has been suggested that cobalt ions occupying surface octahedral sites of γ-Al_2O_3 are reducible, while cobalt ions occupying tetrahedral sites are nonreducible (6). At lower calcination temperatures, filling of the octahedral sites is more favorable. Filling of the tetrahedral sites of γ-Al_2O_3 may be enhanced by an increase in calcination temperature (6). It is suggested, based on this study, that this process can also be enhanced by the presence of water vapor. Water vapor may partially hydrate the cobalt oxides and γ-Al_2O_3 support and, thus, facilitate the migration of cobalt ions into tetrahedral sites of γ-Al_2O_3.

CONCLUSIONS

It can be concluded that water vapor has a significant effect on the reduction behavior of $CoRu/Al_2O_3$ catalyst. Added water vapor had little effect on unsupported Co_3O_4 and on peak 1 in TPR of calcined $CoRu/Al_2O_3$, which is assigned to the reduction of large Co_3O_4 particles (similar to bulk Co_3O_4) to Co metal and partial reduction of highly dispersed Co_3O_4 to CoO. However, it had a dramatic influence on peak 2 in TPR of $CoRu/Al_2O_3$, which is assigned to the reduction of Co species that were well dispersed and strongly interacting with the support. At lower water vapor pressures, the shift of peak 2 was probably due to a change or modification of highly dispersed cobalt species in the presence of water vapor. The slight shifts of peak 1 and peak 2 (at higher water vapor pressures) for $CoRu/Al_2O_3$ as well as the reduction peaks for unsupported Co_3O_4 were probably caused only by the small variations in H_2 concentration and total flow rate.

Introduction of water vapor during standard reduction led to a decrease in the degree of reduction of cobalt probably in two ways: (1) inhibition of the reduction of well-dispersed CoO interacting with the alumina support possibly by increasing the Co–alumina interaction; and (2) facilitation of migration of Co ions into probable tetrahedral sites of γ-Al_2O_3 to form a nonreducible ($\leq$900°C) spinel. Such an irreversible spinel formation results in a decrease in the amount of reduced cobalt metal atoms available to catalyze reactions.

ACKNOWLEDGMENT

The authors thank Energy International (a division of Williams International) for financial support of this work.

REFERENCES

1. Iglesia, E., *Appl. Catal. A* **161**, 59 (1997).
2. Brady, R. C., and Pettit, R. J., *J. Am. Chem. Soc.* **103**, 1287 (1981).
3. Anderson, R. B., "The Fischer-Tropsch Synthesis." Academic Press, Orlando, FL, 1984.
4. Kogelbauer, A., Goodwin, J. G., Jr., and Oukaci, R., *J. Catal.* **160**, 125 (1996).
5. Schanke, D., Hilmen, A. M., Bergene, E., Kinnari, K., Rytter, E., Adnanes, E., and Holmen, A., *Catal. Lett.* **34**, 269 (1995).
6. Chin, R. L., and Hercules, D. M., *J. Phys. Chem.* **86**, 360 (1982).
7. Belambe, A. R., Oukaci, R., and Goodwin, J. G., Jr., *J. Catal.* **166**, 8 (1997).
8. Hilmen, A. M., Schanke, D., and Holmen, A., *Catal. Lett.* **38**, 143 (1996).
9. van de Loosdrecht, J., van der Haar, M., van der Kraan, A. M., van Dillen, A. J., and Geus, J. W., *Appl. Catal. A* **150**, 365 (1997).
10. Schanke, D., Hilmen, A. M., Bergene, E., Kinnari, K., Rytter, E., Adnanes, E., and Holmen, A., *Energy Fuels* **10**, 867 (1996).
11. Reuel, R. C., and Bartholomew, C. H., *J. Catal.* **85**, 63 (1984).
12. Reuel, R. C., and Bartholomew, C. H., *J. Catal.* **85**, 78 (1984).
13. Arnoldy, P., and Moulijn, J. A., *J. Catal.* **93**, 38 (1985).
14. Iglesia, E., Soled, S. L., Fiato, R. A., and Via, G. H., *J. Catal.* **143**, 345 (1993).
15. Ho, S. W., Houalla, M., and Hercules, D. M., *J. Phys. Chem.* **94**, 6396 (1990).
16. Kogelbauer, A., Weber, J. C., and Goodwin, J. G., Jr., *Catal. Lett.* **34**, 259 (1995).
17. Ali, S., Chen, B., and Goodwin, J. G., Jr., *J. Catal.* **157**, 35 (1995).
18. Ming, H., and Baker, B. G., *Appl. Catal. A* **123**, 23 (1995).
19. Buchman, L. B., Rautiainen, A., Krause, A. O. I., and Lindblad, M., *Catal. Today* **43**, 11 (1998).

20. van Steen, E., Sewell, G. S., Makhothe, R. A., Micklethwaite, C., Manstein, H., de Lange, M., and O'Connor, C. T., *J. Catal.* **162**, 220 (1996).
21. van't Blik, H. F. J., Koningsberger, D. C., and Prins, R., *J. Catal.* **97**, 210 (1986).
22. Sellmer, C., Decher, S., and Kruse, N., *Catal. Lett.* **52**, 131 (1998).
23. Ernst, B., Bensaddik, A., Hilaire, L., Chaumette, P., and Kiennemann, A., *Catal. Today* **39**, 329 (1998).
24. Jablonski, J. M., Wolcyrz, M., and Krajczyk, L., *J. Catal.* **173**, 130 (1998).
25. Ho, S. W., and Su, Y. S., *J. Catal.* **168**, 51 (1997).
26. Khodakov, A. Y., Lynch, J., Bazin, D., Rebours, B., Zanier, N., Moisson, B., and Chanmette, P., *J. Catal.* **168**, 16 (1997).
27. Martens, J. H. A., van't Blik, H. F. J., and Prins, R., *J. Catal.* **97**, 200 (1986).
28. Keyser, M. J., Everson, R. C., and Espinoza, R. L., *Appl. Catal. A* **171**, 99 (1998).
29. Noronha, F. B., Schmal, M., Nicot, C., Moraweck, B., and Frety, R., *J. Catal.* **168**, 42 (1997).
30. Bessel, S., *Appl. Catal. A* **126**, 235 (1995).
31. Bartholomew, C. H., *Stud. Surf. Sci. Catal.* **64**, 158 (1991).
32. Haddad, G. J., and Goodwin, J. G., Jr., *J. Catal.* **157**, 25 (1995).
33. Rothaemel, M., Hanssen, K. F., Blekkan, E. A., Schanke, D., and Holmen, A., *Catal. Today* **38**, 79 (1997).
34. Rothaemel, M., Hanssen, K. F., Blekkan, E. A., Schanke, D., and Holmen, A., *Catal. Today* **40**, 171 (1998).
35. van't Blik, H. F. J., and Prins, R., *J. Catal.* **97**, 188 (1986).
36. Richardson, J. T., and Vernon, L. W., *J. Phys. Chem.* **62**, 153 (1958).
37. Cimino, A., Lojcono, M., and Schiavello, M., *J. Phys. Chem.* **79**, 243 (1975).
38. Goodwin, J. G., Jr., *Prepr. ACS Div. Petr. Chem.* **36**, No. 1, 156 (1991).
39. Schanke, D., Vada, S., Blekkan, E. A., Hilmen, A. M., Hoff, A., and Holmen, A., *J. Catal.* **156**, 85 (1995).
40. Vada, S., Hoff, A., Adnanes, E., Schanke, D., and Holmen, A., *Top. Catal.* **2**, 155 (1995).
41. Hurst, N. W., Gentry, S. J., Jones, A., and McNicol, B. D., *Catal. Rev. Sci. Eng.* **24**, 233 (1982).
42. Malet, P., and Caballero, A., *Chem. Soc. Faraday Trans. 1* **84**, 2369 (1988).
43. Zielinski, J., *Catal. Lett.* **32**, 47 (1995).
44. Zielinski, J., *Catal. Lett.* **12**, 389 (1992).